Heat Mass Transfer (2017) 53:439–450
DOI 10.1007/s00231-016-1831-4

ORIGINAL

Inverse estimation of near-field temperature and surface heat flux via single point temperature measurement

Chen-Wu Wu[1] · Yong-Hua Shu[1] · Ji-Jia Xie[1] · Jian-Zheng Jiang[1] · Jing Fan[1]

Received: 13 December 2015 / Accepted: 2 May 2016 / Published online: 13 May 2016

Abstract A concept was developed to inversely estimate the near-field temperature as well as the surface heat flux for the transient heat conduction problem with boundary condition of the unknown heat flux. The mathematical formula was derived for the inverse estimation of the near-field temperature and surface heat flux via a single point temperature measurement. The experiments were carried out in a vacuum chamber and the theoretically predicted temperatures were justified in specific positions. The inverse estimation principle was validated and the estimation deviation was evaluated for the present configuration.

List of symbols

A	Cross-section area
b	Height
V	Volume
l	Length, distance
h	Convective heat exchange coefficient
E	Energy, thermal energy
q	Heat flux, thermal energy flux
T	Temperature
t	Time
x, y, z	Cartesian coordinates
n	Directional vector
ρ	Density
c	Specific heat capacity
C	Heat capacity
k	Thermal conductivity ε surface emissivity
σ	Stephan-Boltzmann constant
Δ	Differentiation of a variable
δ	Variation of a function
C1, C2	Constants

Subscripts

conn	Connecting items
e	Environment
f	Fluid
al	Aluminum
cu	Copper
supp	Supporting parts
v	Virtual, partial derivative

1 Introduction

Recently, a space thermal environment measurement work challenged the authors with great operation constrains. That is, the near-field temperature and the surface heat flux need to be estimated based on the temperature history of a single point at the wall of the near structure. At the same time, the temperature sensor was packaged in a measurement device of relative big heat capacity to guarantee its survival, as shown in Fig. 1. One can image that there inevitably exist heat energy exchange between the measurement device and the near structure because of the necessary installation contact. Although, such heat transfer could be greatly reduced through some thermal insulation design, for which the Silicon Rubber sealing ring and Polytetrafluoroethylene (PTFE) washer working as the interfaces between the device and the near structure, i.e. the aluminum plate, are all of low thermal conductivity.

✉ Chen-Wu Wu
chenwuwu@imech.ac.cn

✉ Jing Fan
jfan@imech.ac.cn

[1] Institute of Mechanics, Chinese Academy of Sciences, No. 15 BeisihuanXi Road, Beijing 100190, China

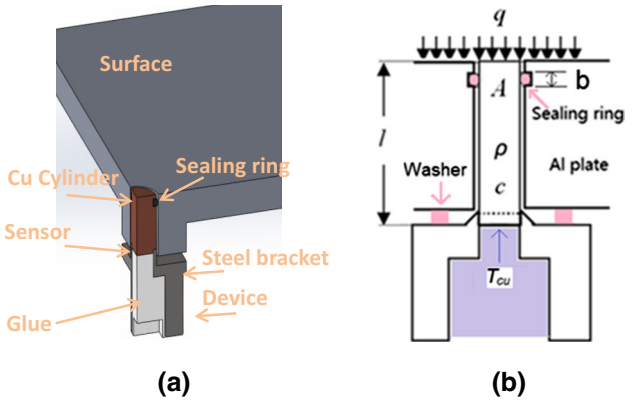

Fig. 1 **a** Quarter sketch and **b** sectional drawing of the device and structure

Theoretically, the near-field temperature and the unknown surface heat flux could be estimated based on the thermal energy deposited in the measurement device. Of course, the effects of the heat exchange between the device and the near structure should be modified by some mathematical methods. One can understand that this is actually an inverse problem of heat conduction with surface heat flux boundary condition [9–12].

Generally speaking, the inverse estimation of thermal boundary conditions has always attracted much research [2, 4, 7, 8, 13–15, 17, 20, 21, 24, 27, 33, 34], as many industry processes require the determination of unknown thermal conditions [3, 22, 23, 25, 26, 28–32].

One would quickly find out that the present work resemble to those on surface heat flux recovery based on inner wall temperature tests, for which there are two classic methods of so called Sequence Function Method (SFM) [6, 18] and Conjugate Gradient Method (CGM) [1, 5, 16, 19]. The SFM is commonly used step by step to inversely calculate the surface heat flux at every instant based on the diffusion characteristic of the transient Fourier heat conduction equations, i.e., the temperature gradient is related to the temperature change rate through the thermal diffusivity. In comparison, the CGM regards the inverse estimation as an optimization problem to approach the real surface heat flux boundary condition and, the algorithm of iterative regularization is used to look for the optimized solution. In almost all of the surface flux inverse methods, several temperature test points on the structure wall are necessary and multiple iterations are needed to obtain the solution to the inverse problem.

However, sometimes we hope to recover the surface heat flux boundary condition through as less temperature test points as possible, even if only one test point is available as aforementioned. Moreover, one might also hope to quickly obtain a good estimation on the surface heat flux boundary condition with as less calculation time expense as possible. That's also the very reason why the device as shown in Fig. 1 had been designed and applied. To be noted again that, the influence of the heat exchange between the measurement device and the near structure is significant during the test. Therefore, with a single point temperature history being known, the inverse estimation of near-field temperature and surface heat flux should be carried out by considering the interfacial heat exchange.

In the present work, a concept was firstly developed to inversely estimate the near-field temperature as well as the surface heat flux for the transient heat conduction problem under the unknown heat flux boundary condition. And the mathematical formula was derived for the inverse estimation of the near-field temperature and surface heat flux. Then, the experiments were carried out in a vacuum chamber and the temperatures measured in certain positions to justify the theoretical prediction. Finally, the inverse estimation principle was validated and the estimation deviation was evaluated based on the difference in that of the theoretical and experimental temperatures at specific locations.

2 Inverse estimation concept and mathematical formula

As shown in Fig. 1, the measurement device is installed in the aluminum plate and the device is mainly composed of the copper cylinder, steel holder and the glue filled in the holder. The temperature sensor is fixed centrally to the back face of the copper cylinder. The front face of the copper cylinder is aligned with the aluminum plate surface, both of which are under the action of a unknown heat flux q(t). In the application of interest, q(t) is very flat over the surface area much greater than the front-end surface of the cylinder, i.e. q(t) is independent of the coordinates along the surface.

The heat conduction equation for both the device and the aluminum plate could be written as

$$\frac{\partial}{\partial \mathrm{x}}\left(k\frac{\partial T}{\partial x}\right)+\frac{\partial}{\partial \mathrm{y}}\left(k\frac{\partial T}{\partial y}\right)+\frac{\partial}{\partial \mathrm{z}}\left(k\frac{\partial T}{\partial z}\right)=\rho c\frac{\partial T}{\partial t}. \quad (1)$$

wherein, x, y and z are Cartesian Coordinates, T is temperature, t is time; k is the thermal conductivity of the material, ρ is the density and c is the specific heat capacity.

The thermal boundary conditions on the front faces of both the device and the aluminum plate are

$$-k\frac{\partial T}{\partial n}=q. \quad (2)$$

wherein, n refers to the outward unit vector normal to the surface.

The thermal boundary conditions on the other surfaces are of the convective heat diffusion

$$-k\frac{\partial T}{\partial n} = \mathrm{h}\left(\mathrm{T}_f - \mathrm{T}\right), \tag{3}$$

as well as the radiation heat diffusion

$$-k\frac{\partial T}{\partial n} = \varepsilon\sigma\left(T_e^4 - T^4\right). \tag{4}$$

where h is convective heat transfer coefficient, ε is the surface emissivity, $\sigma = 5.67 \times 10^{-8}$ W/m^{-2} K^{-4} is the Stephan-Boltzmann constant, T_f is the fluid temperature flowing through the surface and T_e is the ambient temperature. In the actual experiment, the convection and radiation only lead to very small heat diffusion and their effects is negligible.

Now, this is the question, as the surface heat flux q(t) is unknown and need to be inversely estimated through the temperature history $T_{cu}(t)$ of the test point at the back face of the copper cylinder of the device as shown in Fig. 1b. Furthermore, we also need to predict the near-field temperature of the aluminum plate.

Ideally, if there is no heat exchange between the measurement device and the aluminum plate, one can use the thermal energy deposited in the device to calculate the surface heat flux and then the temperature of the aluminum plate. For such case, the temperature field of the device could be roughly computed by exerting the thermal boundary

$$T = T_{cu}, \tag{5}$$

on the heat conduction Eq. (1) of the copper cylinder as the temperature gradient in the copper cylinder is very small in the present work.

However, there is inevitable heat exchange between the device and the aluminum plate because of the installation contact. As for every contacting region, one can write the heat transfer rate across the contact interface as

$$k_+\frac{\partial T_+}{\partial n} = k_-\frac{\partial T_-}{\partial n}. \tag{6}$$

Wherein, the subscripts "+" and "−" refer the two sides across the contacting interface.

Now that, we have to separate the thermal energy due to lateral heat conduction from the total thermal energy that account for the temperature elevation of the device. The primary concept developed herein is described as following.

First of all, as for a certain assemble of the device and the aluminum plate, the temperature increment in infinitesimal timespan of the test point at the copper cylinder of the device $\Delta T_{cu}(t)$, and that of the aluminum plate $\Delta T_{al}(t)$ should be some functional of the surface heat flux q(t), i.e.,

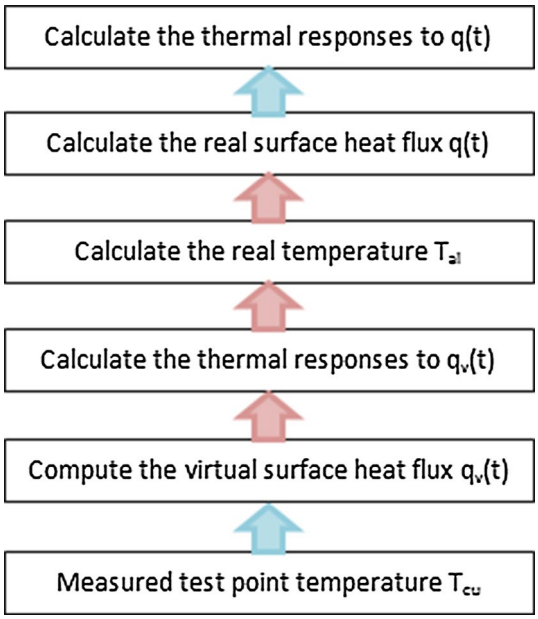

Fig. 2 Sketch for the recovery algorithm

$$\Delta T_{cu}(t) = f_1(q(t)), \tag{7}$$

and

$$\Delta T_{al}(t) = f_2(q(t)). \tag{8}$$

Wherein, $T_{cu}(t)$ refers to the temperature history of the test point at the copper cylinder of the device, and $T_{al}(t)$ is the temperature history of the aluminum plate.

Once $T_{cu}(t)$ is obtained through test, it could be used as temperature boundary for the heat conduction equation on the device and, an virtual temperature field of the device could be calculated at every instant with temporarily supposing there is no heat exchange between the device and the aluminum plate. The virtual thermal energy deposited in the device E(t) could be obtained by simple integral over the device

$$E(t) = \iint (\rho c)_{cu} dT_{cu} dV, \tag{9}$$

and an virtual surface heat flux be obtained as

$$q_v(t) = (1/A_{cu})(dE(t)/dt). \tag{10}$$

While, actually, such virtual surface heat flux should differ from the real surface heat flux by

$$q_v(t) = q(t) + \delta q(t). \tag{11}$$

Similarly, if the virtual surface heat flux [q(t) + δq(t)] is exerted on the front faces of both the device and the aluminum plate, the temperature increment in infinitesimal timespan of the test point at the copper cylinder of the

device $\Delta T_{cu\_v}(t)$, and that of the aluminum plate $\Delta T_{al\_v}(t)$ should be

$$\Delta T_{cu\_v}(t) = f_1(q(t) + \delta q(t)) \tag{12}$$

and

$$\Delta T_{al\_v}(t) = f_2(q(t) + \delta q(t)). \tag{13}$$

When the heat exchange between the device and the aluminum plate is small enough, then δq(t) should also be slight and the right hands of Eqs. (12) and (13) could be approximated by Taylor expansion theorem as

$$\Delta T_{cu\_v}(t) = f_1(q(t)) + f_{1,q}\delta q(t), \tag{14}$$

and

$$\Delta T_{al\_v}(t) = f_2(q(t)) + f_{2,q}\delta q(t), \tag{15}$$

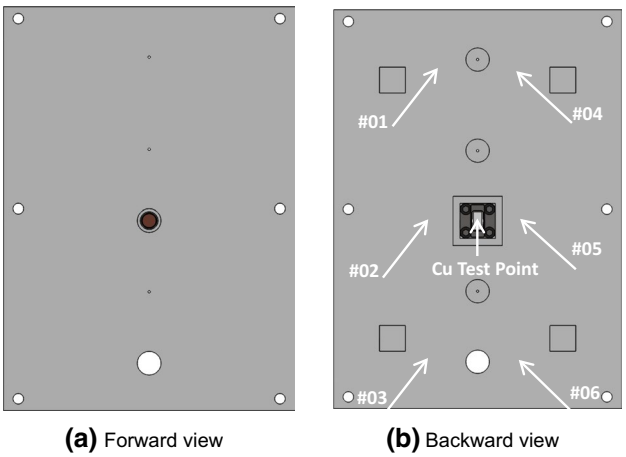

Fig. 3 The experimental set up

respectively. Where, $f_{1,q}$ and $f_{2,q}$ means partially derivative of f_1 and f_2 to q(t), respectively.

Divide Eq. (14) by Eq. (7), and (15) by (8), one can get

$$\Delta T_{cu\_v}(t)/\Delta T_{cu}(t) = 1 + \left(f_{1,q}/f_1\right)\delta q(t) \tag{16}$$

and

$$\Delta T_{al\_v}(t)/\Delta T_{al}(t) = 1 + \left(f_{2,q}/f_2\right)\delta q(t), \tag{17}$$

respectively.

If the temperature dependency of the material properties and the temperature gradient through its thickness are ignored in the transient heat conduction equation [12], one can quickly write the relationship between the temperature increment of the aluminum plate of thickness l_{al} and the surface heat flux q(t) as

$$(\rho c)_{al} l_{al} \Delta T_{al}(t) = q(t). \tag{18}$$

Therein, $(\rho c)_{al}$ is the heat capacity of unit volume aluminum. It is noteworthy that Eq. (18) holds really well because that the heat exchange between the device and the aluminum plate is too small to change the temperature of the aluminum plate by the contact heat conduction.

With considering the effects of the steel holder and filling glue of the device on the solution to the one dimensional transient heat conduction problem [12], we can also relate the test point temperature at the copper cylinder to the surface heat flux q(t) as

$$\left((\rho c)_{cu} l_{cu} A_{cu} + \left(k_{supp} A_{conn}/\sqrt{\pi \alpha_{supp} \times 1}\right)\right)\Delta T_{cu}(t) = q(t) A_{cu}. \tag{19}$$

Wherein, l_{cu} and A_{cu} is the length and cross section area of the copper cylinder of the device, respectively; A_{conn} is the effective connected area between the copper cylinder and the supporting part, k_{supp} and $\alpha_{supp} = k_{supp}/(\rho c)_{supp}$ refers to

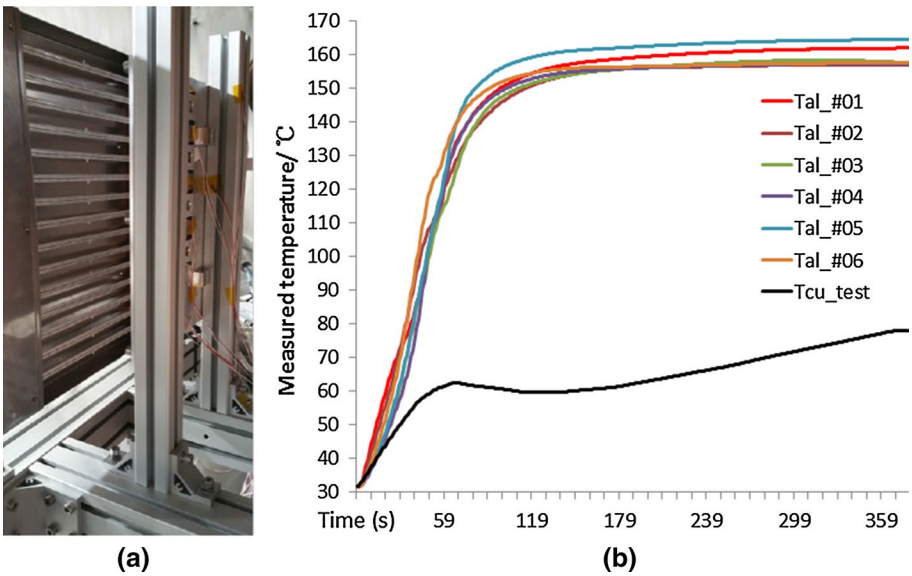

Fig. 4 **a** Experimental set up and **b** temperatures

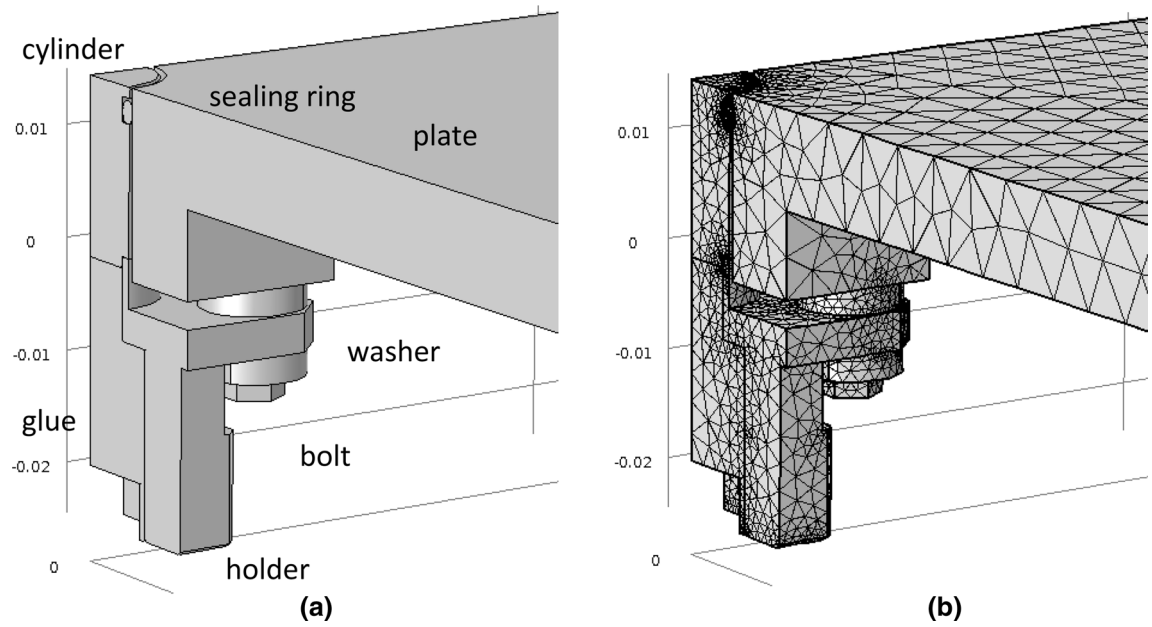

Fig. 5 **a** Geometry model and **b** mesh model of the device and the plate

Table 1 Thermal property of the materials

	ρ (Kg/m^3)	c (J/Kg K)	k (W/m K)
Plate	2700	900	165
Cylinder	8700	385	400
Sealing ring	2000	1700	0.3
Glue	2200	700	0.5
Holder, Bolt	7850	475	15
Washer	2200	1000	0.2

the effective thermal conductivity and effective thermal diffusivity of the supporting parts, respectively. The supporting parts include the steel holder, filling glue and the effective contribution from heat exchange between the device and the aluminum plate. It is noteworthy that the difference in temperature of the device and the aluminum plate is almost stable during the stage of interest in the actual experiment to be described in the following section. Thus, the contribution from the heat exchange between the device and the aluminum plate is independent of the temperature. Therefore, the coefficient term in the parentheses of the left hand side of Eq. (19) should approximately be constant if the temperature dependency of the material properties is ignored.

Then the formula (18) and (19) indicate that, if the temperature increment is not much great and the material properties are not changed so much, f_1 and f_2 are both linear function of q(t), that is

$$f_1(q(t)) = C_1 q(t), \tag{20}$$

and

$$f_2(q(t)) = C_2 q(t). \tag{21}$$

Thus, $f_{1,q}/f_1 = f_{2,q}/f_2 = 1/q(t)$, and now the left hand of Eq. (16) is identical to the left hand of (17), that is

$$\Delta T_{cu\_v}(t)/\Delta T_{cu}(t) = \Delta T_{al\_v}(t)/\Delta T_{al}(t). \tag{22}$$

Immediately, we can get

$$\Delta T_{al}(t) = \Delta T_{al\_v}(t) \times \Delta T_{cu}(t)/\Delta T_{cu\_v}(t). \tag{23}$$

Wherein, $\Delta T_{cu0}(t)$ can be determined directly by the temperature $T_{cu}(t)$ of the test point at the copper cylinder of the device. At the same time, $\Delta T_{al\_v}(t)$ and $\Delta T_{cu\_v}(t)$ could be calculated by solving the heat conduction Eq. (1) under the virtual heat flux boundary condition $[q(t) + \delta q(t)]$. Thereupon, one can obtain $\Delta T_{al}(t)$ through (23).

Take the integral of $\Delta T_{al}(t)$ over the time, one can quickly calculate the temperature of the aluminum plate $T_{al}(t)$ in response to the real surface heat flux boundary q(t). Finally, one can get the real heat flux by divide Eq. (18) by time increment as

$$q(t) = C \times (dT_{al}/dt). \tag{24}$$

Wherein, $C = (\rho c)_{al} l_{al}$ is the heat capacity of aluminum plate of unit area.

3 Inverse estimation algorithm

According to the recovery concept and the mathematical formula, the inverse estimation algorithm could be

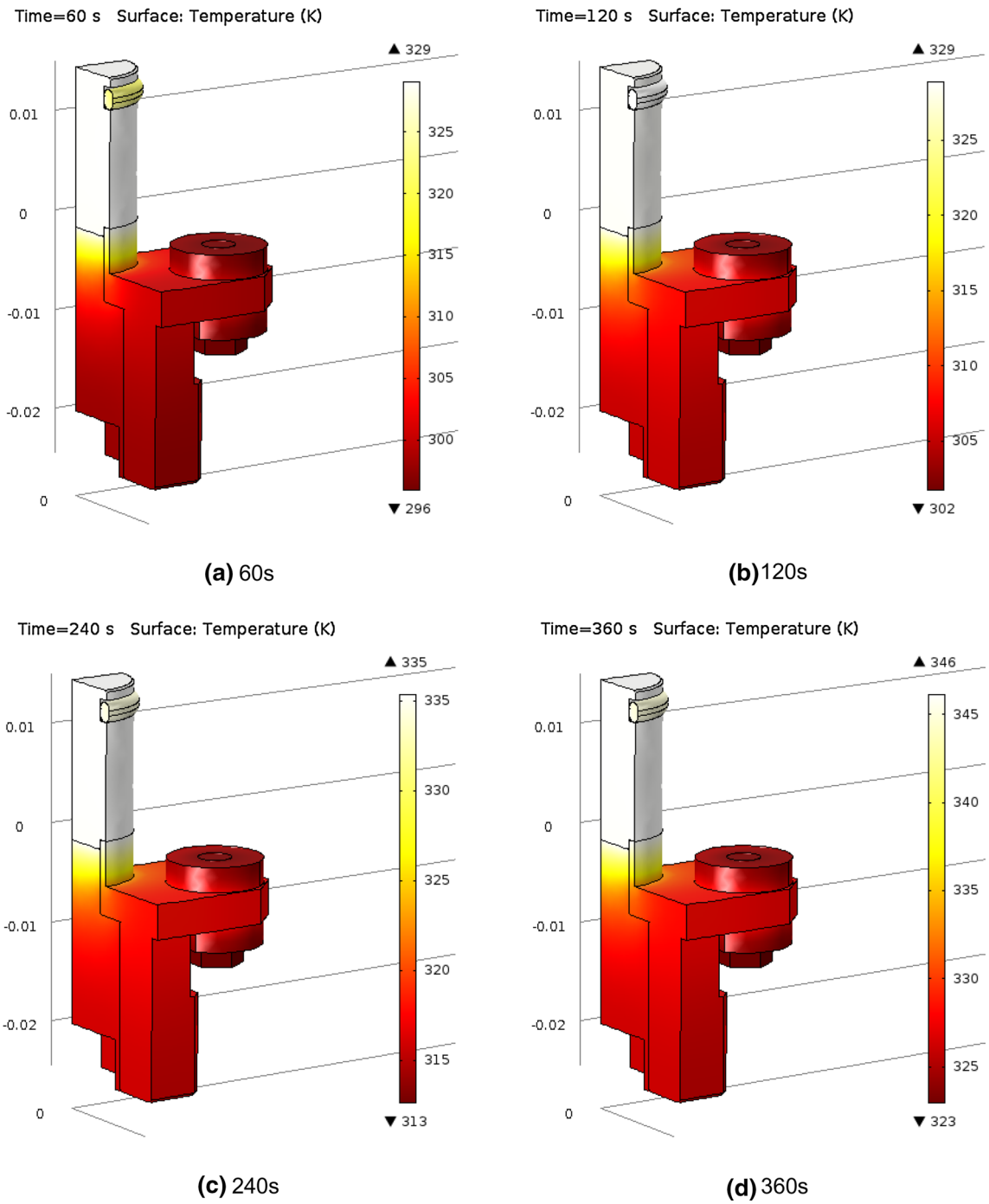

Fig. 6 Temperature profiles (in K) at some instants

demonstrated by Fig. 2. For the recovery algorithm as shown in Fig. 2, the basic procedures for the inverse estimation are described as following.

1. Take the test point temperature history T_{cu} as thermal boundary condition and solve the Eq. (1) only for the device by Finite Element Method. Get the temperature field for the device at every certain instant. Take integral of thermal energy over the device to get the total deposited heat E(t) in the device. Calculate the virtual surface heat flux through Eq. (10).
2. Apply the virtual surface heat flux $q_v(t)$ to the front face of both the device and the aluminum plate and solve numerically the Eq. (1) for the assembly of the device and aluminum plate, in which the heat exchange between the device and the aluminum plate is involved.

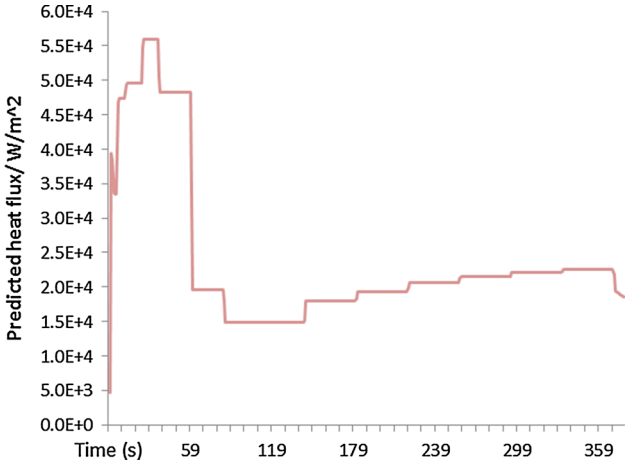

Fig. 7 The virtual surface heat flux (W/m^2)

Get the virtual temperature histories T_{cu_v} (t) and T_{al_v} (t).

3. Apply the virtual temperature histories T_{cu_v} (t) and T_{al_v} (t) to Eq. (23) and get T_{al} (t).
4. Use Eq. (24) to get the real surface heat flux $q(t) = C \times (dT_{al}/dt)$.
5. Apply the estimated real heat flux boundary condition to the assembly of the device and the aluminum plate and solve the Eq. (1) again to get the calculated temperature of the test point. Compare the computed temperature and measured temperature of the test point to check the estimation error.

4 Case study and experimental validation

The near structure, i.e. the aluminum plate and the measurement device are shown in Fig. 3, in which the Fig. 3a shows the forward view and Fig. 3b the backward view, respectively. In the experiment conducted in a vacuum chamber, the Infrared heater was used to irradiate the front face of the assembly of the device and the aluminum plate as shown in Fig. 4a. The electrical current is altered manually to realize certain heat flux fluctuation.

The temperatures are monitored and recorded at the test point in the device and some referenced points on the aluminum plate. The typical temperature histories are shown in Fig. 4, in which the lowest curve represents the temperature of the test point at the back face of the copper cylinder in the device and the other curves of the points at the aluminum plate. It is indicated that the temperature histories are rather similar for those points at the aluminum plate, which indicates that the Infrared heater had provided an evenly heating over the surface. Moreover, the aluminum plate temperature approaches to the maximum in about 60 s and, then stabilizes for several hundred seconds. In comparison, the test point temperature increase with a relative lower rate than the aluminum plate and, it decreases obviously after 60 s and finally increase slowly when the aluminum plate temperature stabilizes. This shows that there is complex heat exchange between the aluminum plate and the device.

While now, we need to intentionally overlook the knowledge of the aluminum plate temperature and, use only the temperature history of the test point at the copper cylinder to inversely estimate the aluminum plate temperature as well as the unknown surface heat flux. According to the theoretical concept as aforementioned, the geometry model and the mesh model for Finite Element analysis are set up as shown in Fig. 5.

The main material parameters used in the Finite Element Analysis are listed in Table 1, in which ρ, c and k are the density, specific heat capacity and thermal conductivity.

The first step is to solve the heat conduction Eq. (1) only for the device with the specified temperature boundary condition (5) exerted on all the nodes of the copper cylinder, for which the temperature T_{cu} was replaced with T_{cu_test} as represented by the lowest curve in Fig. 4b. The calculated temperature profiles of the device at some instants are shown in Fig. 6.

Make an integral of the thermal energy throughout all of the device parts, one can calculate the deposited heat E(t) in the device at every instant. Then a virtual surface heat flux could be obtained via Eq. (10) as shown in Fig. 7. Of course, we should know that, the virtual heat flux shown in Fig. 7 is different from the real heat flux in the extra contribution resulted from the thermal energy exchange between the device and the aluminum plate as indicated by (6), although the difference might be slight as the thermal conductivity of the washer materials is very low.

The second step is to solve the heat conduction Eq. (1) for the assembly of the device and the aluminum plate with regarding the virtual surface heat flux shown in Fig. 7 as the thermal boundary conditions. And the computed temperature profiles for both the device and the aluminum plate are shown in Fig. 8. One can see that the aluminum plate temperature is rather uniform except for the regions closely adjacent to the device. Further, the temperature histories of the point at the back face of the copper cylinder and that of the aluminum plate are represented by the curves displayed in Fig. 9. The temperature histories indicated by the curves in Fig. 9 are apparently different from the experimental results as aforementioned, which is resulted from the fact that the virtual surface heat flux is different from the real one.

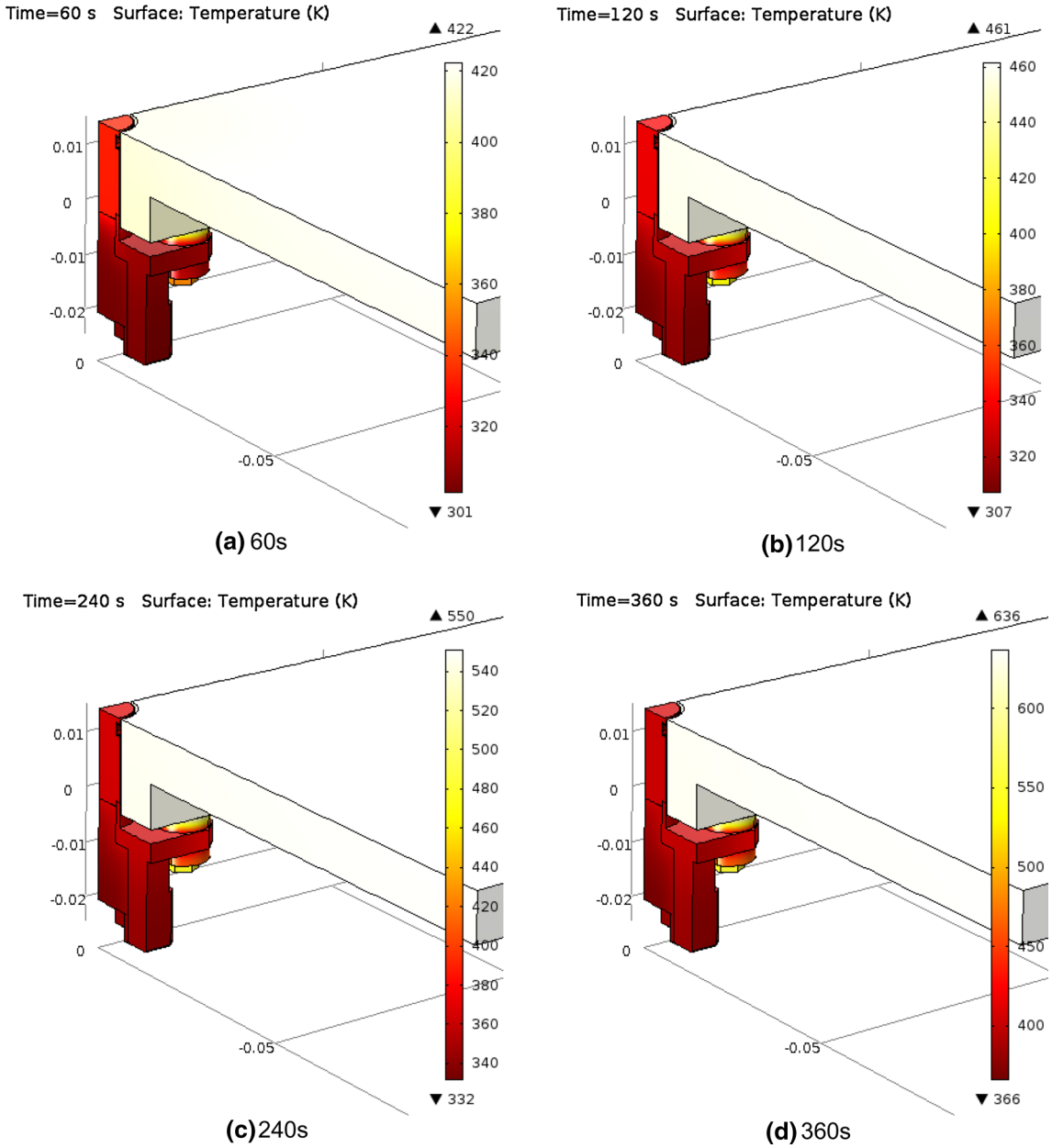

Fig. 8 Temperature (in K) profiles of assembled device and aluminum plate under virtual heat flux

The third step is to calculate the temperature history of the aluminum plate under the action of the real surface heat flux via the formula (23). The predicted temperature of the aluminum plate in comparison to the experimental outcomes is graphed in Fig. 10. The dashed curve in Fig. 10 represents the inversely estimated temperature of the aluminum plate, while the continuous curves refer to the experimentally measured temperatures of the aluminum plate. One can see that the predictions match almost well the experimental outcome, with the estimated temperature being a little higher than the test values. This slight difference might be partially due to that fact that the infrared heater is eventually of finite dimensions, which should have led to a space distribution of surface heat flux. Always, the real heat flux around the edges should be a little lower than that close to the center in comparison to the theoretically assumed absolute even heating over the front-end surface of the aluminum plate. That is to say, the theoretical prediction might have slightly overvalued the total thermal energy, in particular during the heating stage.

Thereafter, one can obtain the estimation of the real surface heat flux by utilizing formula (24) as shown in Fig. 11, in which the negative values of the heat flux is largely related to the configuration of the device other than numerical error. According to the Eq. (24), the negative heat flux imply

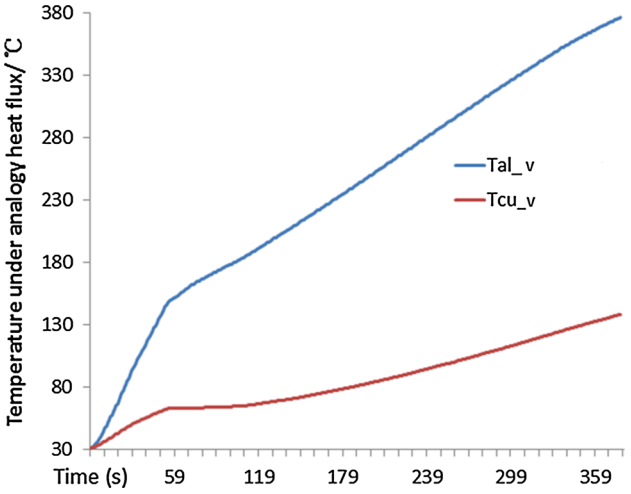

Fig. 9 Temperature (in °C) histories of test point and aluminum plate under virtual heat flux

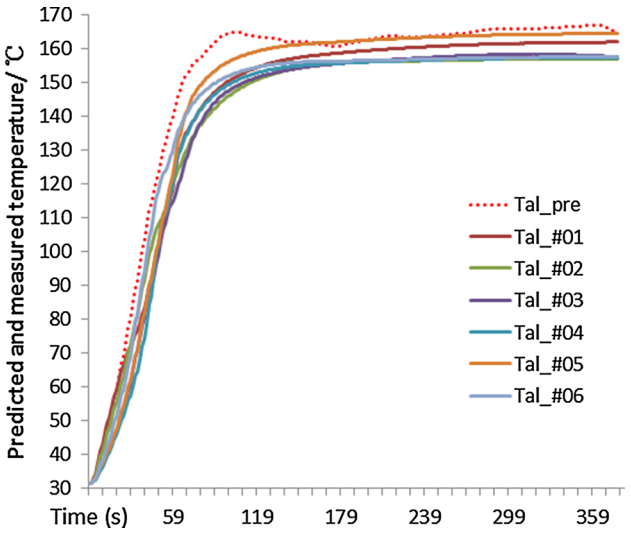

Fig. 10 Aluminum plate temperatures by measurement or prediction

decreasing in temperature of the aluminum, i.e. $\Delta T_{al}(t)$ is negative at that time as indicated in Fig. 10. Moreover, the Eq. (23) tells that $\Delta T_{al}(t) = \Delta T_{al\_v}(t) \times \Delta T_{cu}(t)/\Delta T_{cu\_v}(t)$, in which the $\Delta T_{al\_v}(t)$ and the $\Delta T_{cu\_v}(t)$ are always positive according to the results represented by the curves in Fig. 9. Thus, the negative $\Delta T_{al}(t)$ should be resulted from the negative $\Delta T_{cu}(t)$ at that time, which could be found in Fig. 4b. The temperature history $T_{cu}(t)$ of the test point at the device indicates an apparent trough around the instant t = 120 s and a downslope tendency after t = 360 s, as shown by the black curve in Fig. 4b. This is most probably due to the heat loss conducted from the copper cylinder to the steel bracket. Of course, such heat loss could be greatly suppressed by insert thermal insulator between the copper and the steel bracket in the future designing, or even be eliminated by removing the steel bracket from the future configuration of the device.

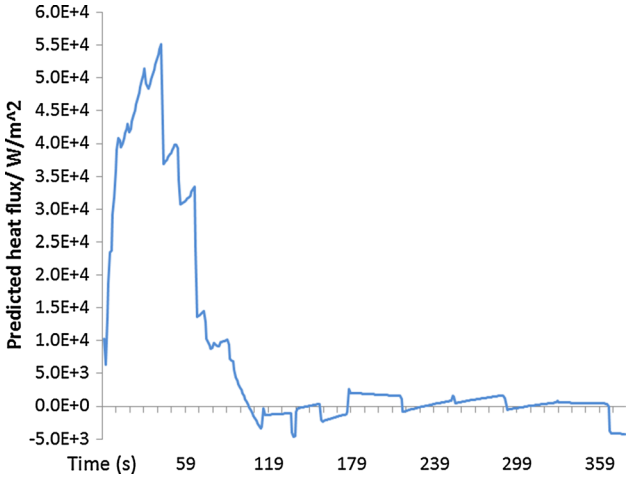

Fig. 11 The estimated surface heat flux (W/m^2)

So, we've arrived at the estimation of the near-field temperature as well as the surface heat flux as an example for the present algorithm. Furthermore, we can do some computational work to justify the correctness of the estimation, though which is not a necessary step.

The forth step is to solve the heat conduction Eq. (1) for the assembly of the device and the aluminum plate with the recovered surface heat flux boundary as shown in Fig. 11. The temperature profiles at some typical instants are shown in Fig. 12, in which the temperature patterns would be found to be similar to that in Fig. 10. While the obviously different magnitudes of the temperature exist as the estimated real surface heat flux is different from the virtual one, in particular after 60 s.

Also, we can compare the calculated temperature history of the test point at the copper cylinder of the device with the experimentally measured one, as shown in Fig. 13. In Fig. 13, the dashed curve represents the predicted temperature of the test point while as the continuous curve is the measured temperature. The largest deviation is about 2 °C, for which the percentage error is about 3.3 %.

5 Error evaluation and discussion

The present inverse estimation algorithm assumed that the temperature gradient through the thickness of both the aluminum plate and copper cylinder is always too slight to be of important meaning. Herein, we'd like to make some investigation on the uncertainty introduced by the above assumption. Let's consider a control volume of thickness dx, for which the one-dimensional equation of energy conversation should be

$$q - k\frac{\partial T}{\partial x} = \rho c\frac{\partial T}{\partial t}. \tag{25}$$

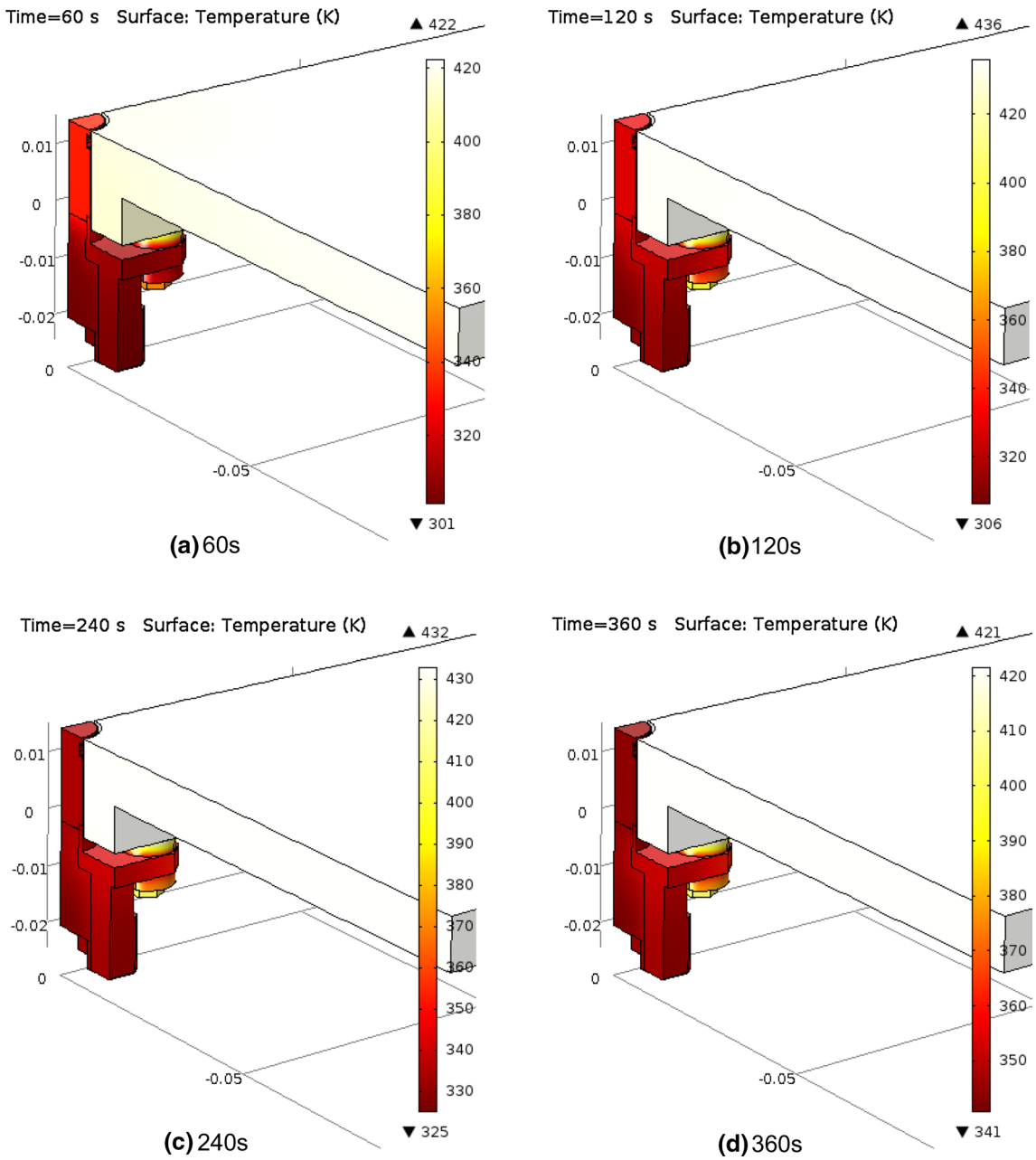

Fig. 12 Temperature profiles of the assembly of the test device and the aluminum under the action of the estimated surface heat flux

For the problem of interest in the present work, the temperature of the copper cylinder as well as the aluminum plate shall increase when q > 0; When the surface heat flux vanishes, i.e. q = 0, the aluminum plate shall be almost steady while the temperature of the copper cylinder decrease or increase with the rate less than that when q > 0. Thus, we always have the inequality

$$\left|\rho c \frac{\partial T}{\partial t}\right| < q_{max}. \tag{26}$$

That means

$$\left|k \frac{\partial T}{\partial x}\right| < q_{max}. \tag{27}$$

Let the maximum temperature difference along the thickness in the copper cylinder or aluminum plate be $\Delta_{\max}$, and the thickness be x. Then, we have

$$\Delta \max < \left|\frac{\partial T}{\partial x}\right| \times x < q_{\max} x/k. \tag{28}$$

Wherein, the peak heat flux q_{max} is about 5.5 e4 w/m^2 as shown in Fig. 11. By using the thermal conductivity

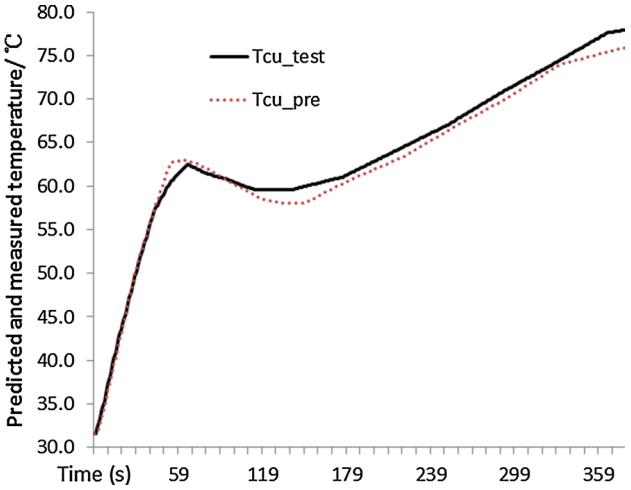

Fig. 13 The predicted and measured temperature (in °C) of the test point

(165 W/mK) and thickness (9 mm) of the aluminum plate, one can obtain the maximum temperature difference along thickness in the aluminum plate $\Delta_{\max}^{Al}$ is less than 3 K. Similarly, by using the thermal conductivity (400 W/mK) and thickness (16 mm) of the copper cylinder, one can obtain the maximum temperature difference along thickness in the copper cylinder $\Delta_{\max}^{Cu}$ is less than 2.2 K. Such error is completely acceptable for the problem we're interested.

However, the algorithm with high order of accurateness should be developed by considering the temperature difference along the thickness for the case that the surface heat flux is largely greater than that of interest in the present work. Moreover, the heat loss due to the heat loss conducted from the copper cylinder to the steel bracket should be suppressed by increasing the thermal resistance between the copper and the steel bracket in the future configuration.

6 Conclusions

The present article develops a concept to predict the near-field temperature as well as inversely estimate the unknown surface heat flux for the transient heat conduction problem with surface heat flux boundary condition.

First, the mathematical formula was derived for the inverse estimation of the near-field temperature and surface heat flux based on variation principle and numerical computation. Then, the typical experiment was carried out in a vacuum chamber and the corresponding inverse estimation was conducted as an example. Finally, the inverse estimation principle was validated and the estimation deviation was evaluated.

The inverse estimation algorithm accounts for the heat conduction within the device, as well as the thermal energy exchange between the device and the near structure. For the present configuration and parameters, the maximum deviation of the predicted temperature from the measured one at the test point is about 2 °C, for which the percentage error is about 3.3 %.

Acknowledgments This work was supported by the National Natural Science Foundation of China (Grant No. 11332011 and No. 11572327). Thanks are also due to Dr. He-Ji Huang, Mr. She Chen and Mr. Hao-Lin Li, et al. for the assistance in conducting the experimental work.

References

1. Hestenes M, Stiefel E (1952) Methods of conjugate gradients for solving linear systems. J Res Natl Bur Stand 49(6):409–436
2. Alifanov M (1972) Solution of an inverse problem of heat conduction by iteration methods. J Eng Phys 26:471–476
3. Diller TE, Hartnett JP, Irvine TF (1993) Advances in heat flux measurements. Adv Heat Transf 23:279–368
4. Chantasiriwan S (1999) Comparison of three sequential function specification algorithms for the inverse heat conduction problem. Int Commun Heat Mass Transf 26(1):115–124
5. Huang CH, Wang SP (1999) A three-dimensional inverse heat conduction problem in estimating surface heat flux by conjugate gradient method. Int J Heat Mass Transf 42:3387–3403
6. Chantasiriwan S (1999) Inverse heat conduction problem of determining time-dependent heat transfer coefficient. Int J Heat Mass Transf 42(23):4275–4285
7. Chen H-T, Lin S-Y, Fang L-C (2001) Estimation of surface temperature in two-dimensional inverse heat conduction problems. Int J Heat Mass Transf 44(8):1455–1463
8. Duda P et al (2003) Solution of multidimensional inverse heat conduction problem. Heat Mass Transf 40:115–122. doi:10.1007/s00231-003-0426-z
9. Chen CO-K et al (2005) Estimation of unknown outer-wall heat flux in turbulent circular pipe flow with conduction in the pipe wall. Int J Heat Mass Transf 48(19–20):3971–3981
10. Chen CO-K et al (2006) Application of the inverse method to the estimation of heat flux and temperature on the external surface in laminar pipe flow. Appl Therm Eng 26(14–15):1714–1724
11. Kowsary F et al (2006) Transient heat flux function estimation utilizing the variable metric method. Int Commun Heat Mass Transf 33(6):800–810
12. Incropera FP, DeWitt DP, Bergman TL, Lavine AS (2007) Fundamentals of heat and mass transfer. Wiley, New York
13. Ijaz UZ et al (2007) Estimation of time-dependent heat flux and measurement bias in two-dimensional inverse heat conduction problems. Int J Heat Mass Transf 50(21–22):4117–4130
14. Daouas N et al (2008) Solution of a coupled inverse heat conduction–radiation problem for the study of radiation effects on the transient hot wire measurements. Exp Thermal Fluid Sci 32(8):1766–1778
15. Mulcahy JM et al (2009) Heat flux estimation of a plasma rocket helicon source by solution of the inverse heat conduction problem. Int J Heat Mass Transf 52(9–10):2343–2357
16. Chen W-L, Yang Y-C (2011) Inverse prediction of frictional heat flux and temperature in sliding contact with a protective strip by iterative regularization method. Appl Math Model 35(6):2874–2886
17. Feng ZC et al (2011) Estimation of front surface temperature and heat flux of a locally heated plate from distributed sensor data on the back surface. Int J Heat Mass Transf 54(15–16):3431–3439

18. Lin DTW, Yang CY, Li JC, Wang CC (2011) Inverse estimation of the unknown heat flux boundary with irregular shape fins. Int J Heat Mass Transf 54(25–26):5275–5285
19. Kameli H, Kowsary F (2012) Solution of inverse heat conduction problem using the lattice Boltzmann method. Int Commun Heat Mass Transf 39(9):1410–1415
20. Liu F-B (2012) Inverse estimation of wall heat flux by using particle swarm optimization algorithm with Gaussian mutation. Int J Therm Sci 54:62–69
21. Mirsephai A et al (2012) An artificial intelligence approach to inverse heat transfer modeling of an irradiative dryer. Int Commun Heat Mass Transf 39(1):40–45
22. Balaji C et al (2013) Incorporating engineering intuition for parameter estimation in thermal sciences. Heat Mass Transf 49:1771–1785. doi:10.1007/s00231-013-1213-0
23. Brittes R, França FHR (2013) A hybrid inverse method for the thermal design of radiative heating systems. Int J Heat Mass Transf 57(1):48–57
24. Mirsepahi A et al (2013) A comparative artificial intelligence approach to inverse heat transfer modeling of an irradiative dryer. Int Commun Heat Mass Transf 41:19–27
25. Bhowmik A et al (2014) Inverse modeling of a solar collector involving Fourier and non-Fourier heat conduction. Appl Math Model 38(21–22):5126–5148
26. De Faoite D et al (2014) Inverse estimate of heat flux on a plasma discharge tube to steady-state conditions using thermocouple data and a radiation boundary condition. Int J Heat Mass Transf 77:564–576
27. Kameli H, Kowsary F (2014) A new inverse method based on Lattice Boltzmann method for 1D heat flux estimation. Int Commun Heat Mass Transf 50:1–7
28. Parwani A et al (2014) Estimation of boundary heat flux using experimental temperature data in turbulent forced convection flow. Heat Mass Transf 9:411–421. doi:10.1007/s00231-014-1421-2
29. Weisz-Patrault D et al (2014) Temperature and heat flux fast estimation during rolling process. Int J Therm Sci 75:1–20
30. Fernandes AP et al (2015) An analytical transfer function method to solve inverse heat conduction problems. Appl Math Model 39(22):6897–6914
31. Li Y et al (2015) Simultaneously estimation for surface heat fluxes of steel slab in a reheating furnace based on DMC predictive control. Appl Therm Eng 80:396–403
32. Qian W et al (2015) Estimation of surface heat flux for ablation and charring of thermal protection material. Heat Mass Transf 8:1–7. doi:10.1007/s00231-015-1653-9
33. Taigbenu AE (2015) Inverse solutions of temperature, heat flux and heat source by the Green element method. Appl Math Model 39(2):667–681
34. Mohebbi F, Sellier M (2016) Estimation of thermal conductivity, heat transfer coefficient, and heat flux using a three dimensional inverse analysis. Int J Therm Sci 99:258–270